

The progenitor set of present-day early-type galaxies

S. Kaviraj^{1*}, J. E. G. Devriendt², I. Ferreras³, S. K. Yi⁴ and J. Silk¹

¹*Department of Physics, University of Oxford, Keble Road, Oxford OX1 3RH, UK*

²*Observatoire Astronomique de Lyon, 9 Avenue Charles André, 69561 Saint-Genis Laval cedex, France*

³*Physics Department, King's College London, Strand, London, WC2R 2LS*

⁴*Center for Space Astrophysics, Yonsei University, 134 Shinchon, Seoul 120-749, Korea*

11 January 2006

ABSTRACT

We present a comprehensive theoretical study, within a fully realistic semi-analytical framework, of the photometric properties of early-type progenitors in the redshift range $0 < z < 1$, as a function of the luminosity and local environment of the early-type remnant at present-day. We find that while larger early-types are generally assembled *later*, their luminosity-weighted stellar ages are typically *older*. In dense environments, ~ 70 percent of early-type systems are in place by $z = 1$ and evolve without major interactions thereafter, while in the field the corresponding value is ~ 30 percent. Averaging across all environments at $z \sim 1$, less than 50 percent of the stellar mass which ends up in early-types today is actually in early-type progenitors at this redshift. The corresponding value is ~ 65 percent in clusters due to faster morphological transformations in the such dense environments. We also develop probabilistic prescriptions which provide a means of *including* spiral (i.e. non early-type) progenitors at intermediate and high redshifts, based on their luminosity and optical (*BVK*) colours. For example, at intermediate redshifts ($z \sim 0.5$), large ($M_B < -21.5$), red ($B - V > 0.7$) spirals have $\sim 75 - 95$ percent chance of being a progenitor, while the corresponding probability for large blue spirals ($M_B < -21.5$, $B - V < 0.7$) is $\sim 50 - 75$ percent. Finally, we explore the correspondence between the *true* progenitor set of present-day early-types and the commonly used ‘red-sequence’, defined as the set of galaxies within the part of the colour-magnitude space which is dominated by early-type objects. While large members ($M_V < -22$) of the ‘red sequence’ trace the progenitor set accurately in terms of numbers and mass, the relationship breaks down severely at fainter luminosities ($M_V > -21$). Hence the red sequence is generally *not* a good proxy for the progenitor set of early-type galaxies.

Key words: galaxies: elliptical and lenticular, cD – galaxies: evolution – galaxies: formation – galaxies: fundamental parameters

1 INTRODUCTION

As ‘end points’ of galaxy merger sequences, early-type galaxies carry important signatures of mass assembly and star formation in the Universe. Deducing their star formation histories (SFHs) therefore contains the key to understanding not only the evolution of these galaxies but characteristics of galaxy formation as a whole. Our view of early-type galaxy formation has developed over the years, away from the classical version of ‘monolithic collapse’ and towards the hierarchical assembly of these objects through mergers and accretion of fragments over a Hubble time, as advocated by the currently popular Λ CDM paradigm of galaxy formation.

Traditionally, the evolution in the properties of early-

type galaxies, for example their optical colours, has been traced by studying early-type populations at progressively higher redshift. However, a fundamental feature of early-type formation in the standard model is that stellar mass that eventually ends up in present-day early-type galaxies is *not entirely* contained in early-type systems at high redshift. Looking *only* at early-type systems at high redshift introduces a *progenitor bias*, which becomes increasingly more severe at higher redshift, as the fraction of early-type progenitors becomes progressively smaller (van Dokkum and Franx 2001, 1996).

In the current era of large scale (optical) surveys e.g. SDSS, COMBO-17, GALEX, MUSYC, GEMS, unprecedented amounts of data spanning a large range in redshift and environment is becoming available, allowing us to study statistically significant numbers of galaxies at various stages

* E-mail: skaviraj@astro.ox.ac.uk

of evolution. A quantitative assessment of progenitor bias is therefore needed to gauge the role of non-early-type progenitors, especially for studies which centre on high redshift.

A central theme of this work is to quantify progenitor bias. This phenomenon has already been studied by van Dokkum and Franx (2001). However, their study employed phenomenological SFHs, with the simple assumption that morphological transformations occur ~ 1.5 Gyrs after the cessation of star formation in a particular galaxy. Our study extends the results of van Dokkum and Franx (2001) by using a fully realistic semi-analytical framework, in which mass assembly and morphological transformation can be followed more accurately in the context of the currently popular Λ CDM paradigm. We study the evolution of the *progenitor set* (galaxies that are progenitors of present-day early-types) with redshift, as a function of the luminosity and environment of the early-type remnant which is left at present-day. We pay particular attention to *spiral progenitors* in the model, since these are routinely excluded from studies of early-type galaxies at high redshift by virtue of their morphology, even though they form an important part of the progenitor set. By comparing the properties (optical colours and luminosities) of spiral progenitors to the general spiral population, we provide a means of correcting for progenitor bias by *including* specific parts of the spiral population at high redshift into the study of early-type evolution.

The plan of this paper is as follows. In Section 2, we quantify the morphology of the progenitor set and map the general properties of elliptical, S0 and spiral progenitors as a function of redshift. In Section 3 we focus exclusively on *spiral progenitors* and compare their photometric properties to the general spiral population. In Section 4 we trace the contribution of galaxies in dense regions (groups and clusters) at high redshift to cluster early-types at present-day. In Section 5 we explore the correspondence between the *true* progenitor set of present-day early-type galaxies and the ‘red-sequence’, defined as the set of galaxies within the part of the colour-magnitude space dominated by early-type objects, which is commonly used as a proxy for the progenitor set (e.g. Bell and GEMS collaboration 2004).

Note that throughout this study we provide *rest-frame* magnitudes for all model galaxies. Unless otherwise noted, the filters used are in the standard Johnson system.

2 DISSECTING THE PROGENITOR SET: MORPHOLOGIES OF PROGENITORS

Early-type galaxies have an assortment of SFHs. Crucial to this study is the *dynamical age* of an early-type galaxy, which we define as the epoch at which its last merger took place. This last merger creates the early-type remnant and imparts its final early-type morphology. As our subsequent analysis of progenitor bias involves morphologies and environments of model galaxies, a brief explanation of the definition of these quantities is necessary.

Galaxy morphology in the model is determined by the ratio of the B-band luminosities of the disc and bulge components which correlates well with Hubble type (Simien and de Vaucouleurs 1986). A morphology index is defined as

$$I = \exp\left(\frac{-L_B}{L_D}\right) \quad (1)$$

such that a pure disc has $I = 1$ and a pure bulge has $I = 0$. Following Baugh et al. (1996), ellipticals have $I < 0.219$, S0s have $0.219 < I < 0.507$ and spirals have $I > 0.507$. This simple prescription is clearly incapable of capturing the complex spectrum of real galaxy morphologies. Therefore, in what follows, ‘spirals’ refer to *all* systems which do not have a dominant spheroidal (bulge) component. Observationally, this includes not only systems with distinctive spiral morphologies, but also peculiar or irregular systems.

Galaxy environments in the model are driven by the mass of the dark matter (DM) halo in which they are embedded. At $z = 0$, DM halo masses greater than $\sim 10^{14} M_\odot$ correspond to ‘cluster’ environments, while halo masses between $\sim 10^{13} M_\odot$ and $\sim 10^{14} M_\odot$ correspond to ‘groups’. All other halo masses correspond to the ‘field’. At higher redshifts these definitions do not strictly hold since the DM halo population is evolving - for example, the largest haloes at $z = 1$ are likely to be roughly half their size at present day (e.g. van den Bosch 2002). We take this mass accretion history into account when specifying the environments of galaxies at high redshift. The mass accretion history is taken from van den Bosch (2002, see their Figure 5).

Figure 1 (top panel) indicates the last merger redshifts of the sample of early-types in the model split by *environment of the remnant* at $z = 0$. The bottom panel in Figure 1 shows histograms of the last merger redshifts shown in the top panel, again split by environment. The inset shows the *fraction* of mergers at a given redshift. In Figure 2 we plot the *average* last merger ages as a function of the luminosity and environment of the early-type remnant at $z = 0$. As expected, we find that, in all environments, larger early-types are *assembled later* (although their stars are generally older (Kaviraj et al. 2005)). Cluster galaxies (at least those brighter than L_*) have significantly larger dynamical ages - morphological transformations in clusters proceed more quickly than in all other environments. This point is more clearly made in Figure 3, where we plot the *cumulative* fraction of early-type galaxies which have already had their last merger. These galaxies have therefore achieved their final ‘early-type’ morphology and are evolving ‘monolithically’. We find that, on average, without reference to environment, only 35 percent of early-type galaxies are in place by $z = 1$ (black line) - the rest are still ‘in pieces’. In terms of morphological transformations cluster environments are *special*, in that early-type morphologies are attained significantly faster in clusters (red curve), with almost 70 percent of early-type galaxies having undergone their last merger by $z = 1$.

Before the last merger occurs, the morphology of the progenitors is *not necessarily early-type*. Figure 4 shows the morphologies of progenitors in *binary* mergers as a function of redshift. Non-binary mergers do happen but are rare, and only take place at redshifts greater than $z \sim 1$. In the local Universe, mergers between early-type progenitors make up less than 20 percent of the merger activity. All other mergers contain at least one spiral progenitor. Mergers involving solely spiral progenitors increasingly dominate at higher redshift and dominate the merger activity beyond $z = 1$.

Having provided a picture of the merger activity within

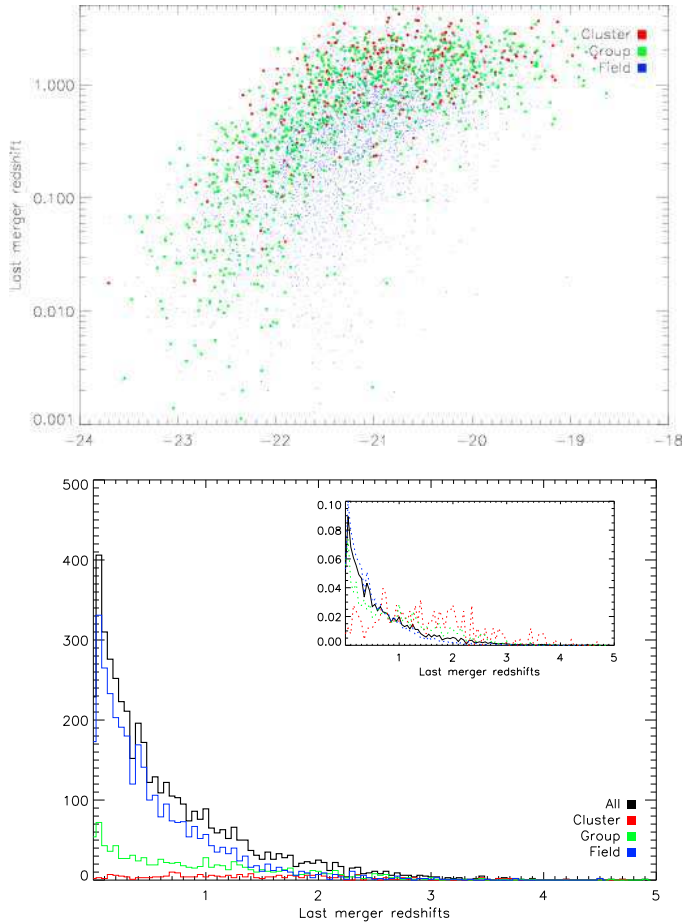


Figure 1. TOP: Last merger redshifts of the sample of early-types in the model split by environment of the remnant at $z = 0$. BOTTOM: Histograms of last merger redshifts shown in the top panel, split by environment. The inset shows the *fraction* of mergers at a given redshift.

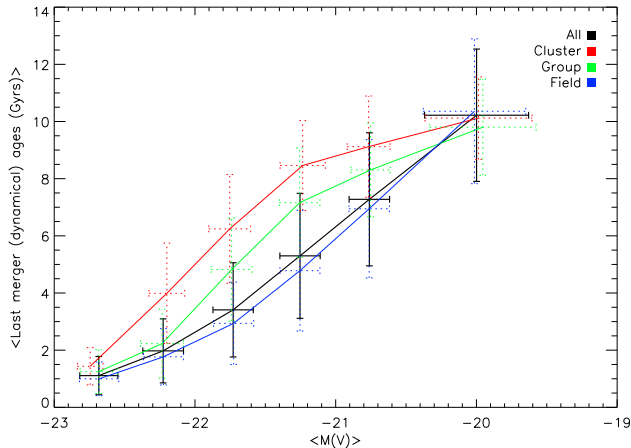


Figure 2. Last merger ages as a function of average luminosity and environment of the early-type remnant at $z = 0$.

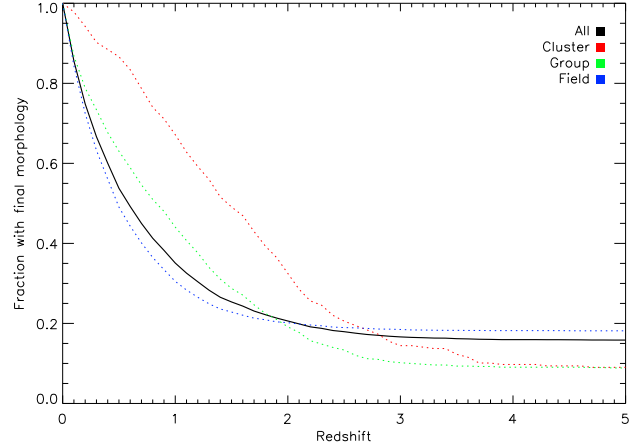


Figure 3. Cumulative fraction of early-type galaxies which have their last merger as a function of redshift.

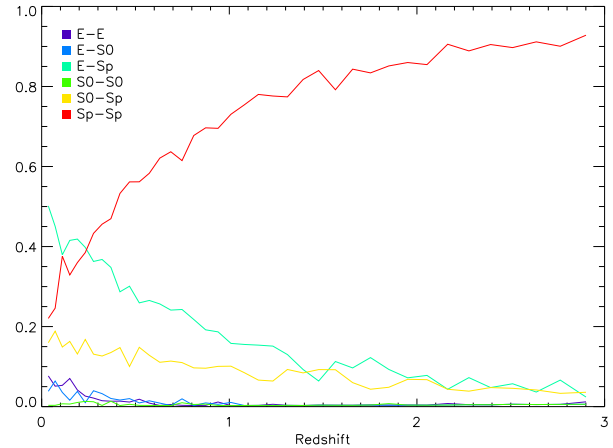


Figure 4. Morphologies of progenitors in binary mergers as a function of redshift. Non-binary mergers do happen but are rare, and only take place at redshifts greater than $z \sim 1.5$. Mergers at intermediate and high redshift are dominated by pairs of progenitors which contain at least one spiral progenitor.

the progenitor set, it is instructive to look at the *fraction* of the progenitor set which is made up of a certain morphological type as a function of redshift. Figures 5 and 6 shows the number and mass fractions contained in progenitors of different morphological types in the redshift range $0 < z < 3$, split by environment and luminosity of the early-type remnant at $z = 0$ respectively. We find that, averaging across all environments, at $z \sim 1$, less than 50 percent of the stellar mass which ends up in early-types today is actually in *early-type progenitors* at this redshift. Faster morphological transformation in cluster environments means that this value is ~ 65 percent in clusters at $z \sim 1$. As a result, looking *only* at early-type galaxies at $z \sim 1$ does not take into account almost half the stellar mass in the progenitor set. In other words, the mass in the progenitor set doubles between $z = 1$ and $z = 0$. A similar result was found by Bell et al. (2004), although they used the optical ‘red sequence’

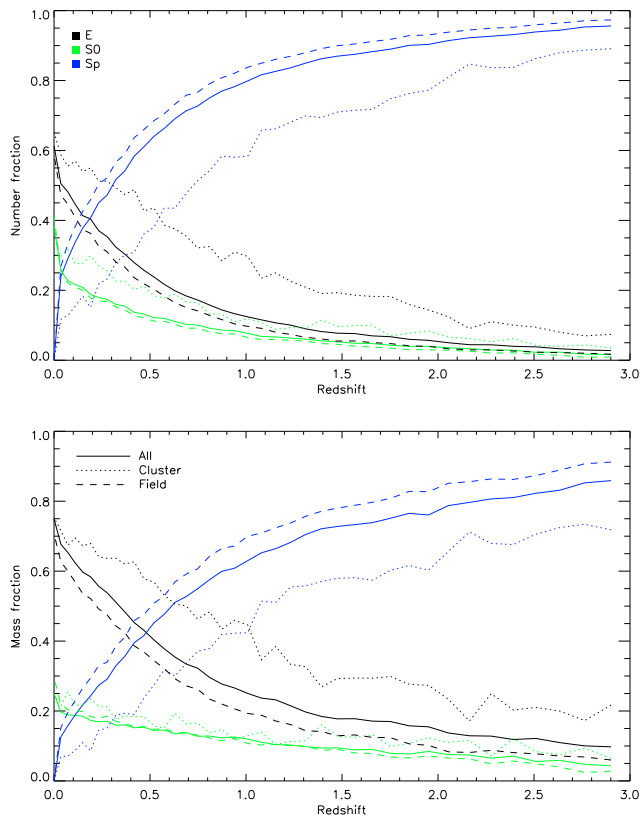


Figure 5. Number (top) and mass (bottom) fractions contained in progenitors of different morphological types in the redshift range $0 < z < 3$, split by environment of the early-type remnant.

in their study, which does not completely correspond to the progenitor set of present-day early-type galaxies (see section 5 below).

The bias does not arise simply because some progenitor mass is not taken into account, but because the age profile of the mass in progenitors of different morphological types tends to vary. We illustrate this point in Figure 7. The top panel shows the average *NUV*-weighted ages of progenitors of different morphological types. The *NUV* weighting, generated using the GALEX (Martin et al. 2005) *NUV* filter, is heavily dominated by stars formed within the last 0.5 to 1 Gyr of look-back time. At all redshifts, early-type progenitors have higher *NUV*-weighted ages, because the mass fraction contributed by recent star formation (RSF) i.e. within the last 1 Gyr is smaller than for spiral progenitors. The differences between elliptical and spiral progenitors are most pronounced at low redshift. The bottom panel shows the fraction of the RSF across the progenitor that is contained in each morphological type. This plot obviously has to be interpreted in conjunction with the mass fractions hosted by each morphological type as a function of redshift. For example, at $z \sim 0.1$, although spiral progenitors host ~ 40 percent of the total RSF in the progenitor set, they only constitute ~ 30 percent of the mass in the progenitor set (see bottom panel of Figure 5). Early-type progenitors (elliptical and S0 taken together) contribute ~ 60 percent of the RSF

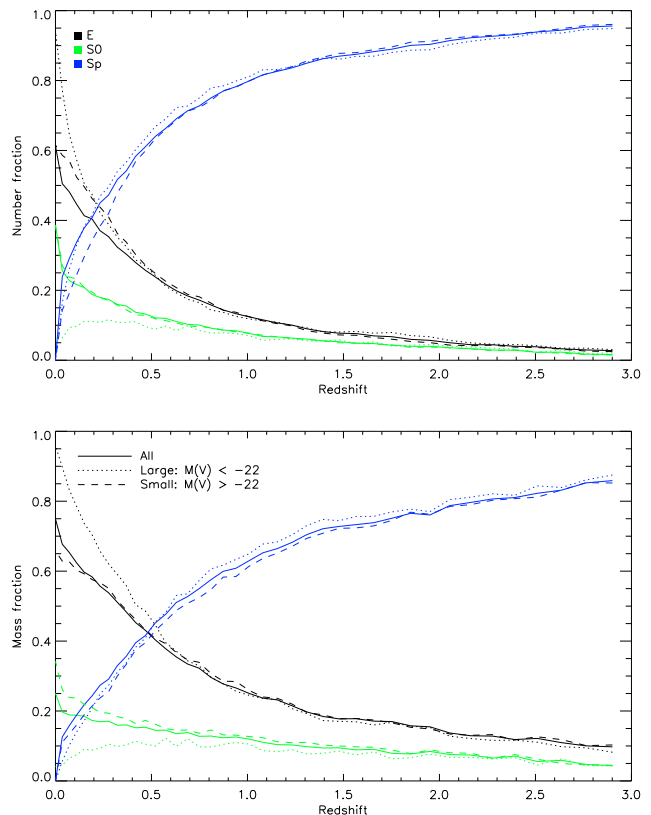


Figure 6. Number (top) and mass (bottom) fractions contained in progenitors of different morphological types in the redshift range $0 < z < 3$, split by luminosity of the early-type remnant.

- but they also constitute ~ 70 percent of the total mass in the progenitor set. Therefore at $z \sim 0.1$ spiral progenitors host 1.5 times the amount of RSF *per unit mass* than their early-type counterparts. At higher redshift the balance of RSF contained in each morphological type moves towards spiral progenitors, partly because they are more spirals in the Universe than early-types.

Figure 7 illustrates that an increasingly larger fraction of RSF in the progenitor set is contained in late-type systems at increasing redshift. In the context of colour-magnitude relations (CMRs), which are often used to age-date early-type populations at all redshifts, the exclusion of spiral progenitors at high redshift biases the CMR towards redder colours and does not give a proper indication of the age of the stellar mass that eventually constitutes present-day early-type galaxies.

3 THE SPIRAL PROGENITORS

One of the aims of this study is to provide a means of *including* spiral populations observed at high redshift which might be early-type progenitors, and thus correct, at least partially, for progenitor bias. We therefore focus on spiral progenitors predicted by the model and compare their photometric properties to the general spiral population.

Providing reasonably accurate prescriptions for finding

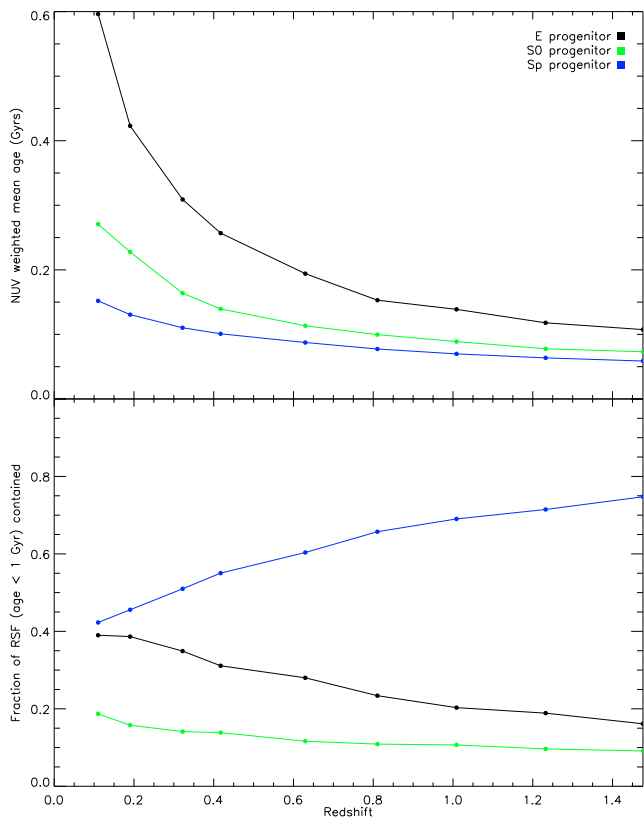


Figure 7. TOP: Average *NUV*-weighted ages of progenitors of different morphological types. The *NUV* weighting is heavily dominated by stars formed in these progenitors within the last 0.5 to 1 Gyr of look-back time. Note that the *NUV* weighting was generated using the GALEX (Martin et al. 2005) *NUV* filter. BOTTOM: The fraction of recently formed stars (age < 1 Gyrs old) across the progenitor set which is contained in progenitors of each morphological type.

progenitors (of any morphology) based on predicted photometry is clearly reliant on the predictions being reasonably representative of the observed data. The correspondence between predictions from GALICS and observed optical photometry (mainly at low redshift) is shown in Hatton et al. (2003, Section 8). The predictions from GALICS produces good agreement to the galaxy luminosity functions observed by the 2dF survey in the B and K bands (Cross et al. 2001). The $(B - V)$ colours of spiral galaxies closely follow the observed data of Buta et al. (1994), both in terms of average values and scatter. The version of the model used in this study is the same as that used in Kaviraj et al. (2005), who calibrated GALICS to accurately reproduce the optical colours of elliptical galaxies in dense environments from $z = 0$ to $z \sim 1.23$. Since our study hinges on photometric predictions at high redshift, we compare, as a further check, in Figure 8, the $(B - V)$ colours of the spiral population in GALICS to recent photometry from COMBO-17 survey (Wolf et al. 2004) in the redshift range $0 < z < 1$. The COMBO-17 sample used is restricted to galaxies which correspond to the GALICS completeness limits in the B and V bands of -18.9 and -19.7 mag respectively.

We find that predicted spiral colours in GALICS cor-

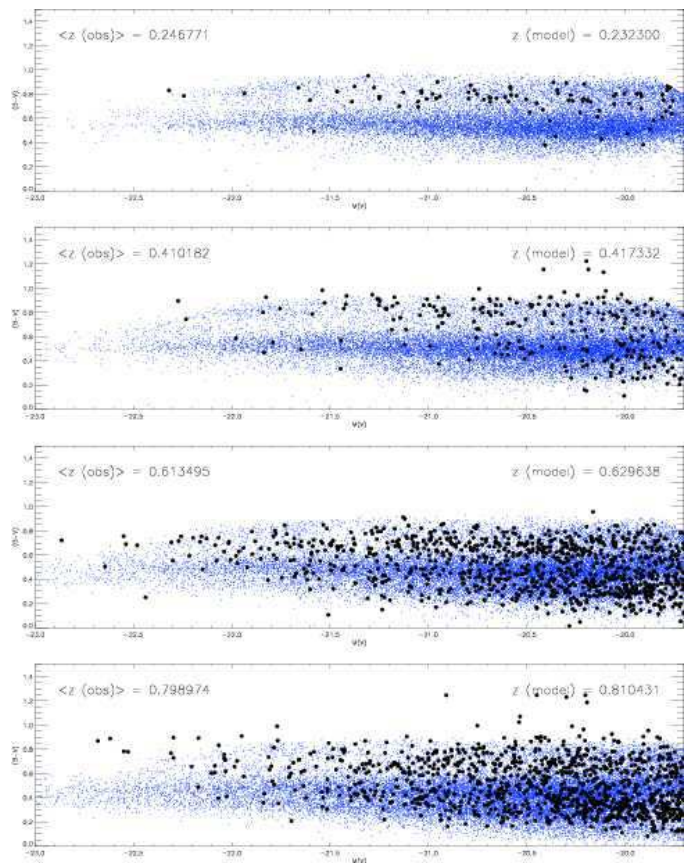


Figure 8. Comparison between the colours of COMBO-17 galaxies and the predicted spiral population in GALICS. The COMBO-17 sample is restricted to galaxies which correspond to the GALICS completeness limits in the B and V bands of -18.9 and -19.7 mags respectively.

respond well to the range of observed $(B - V)$ colours in the COMBO-17 survey in the redshift range $0 < z < 0.8$. Comparison to higher redshifts is not possible because the accuracy of the observed V magnitudes cannot be guaranteed beyond $z \sim 0.7$ (Wolf et al. 2004). However, these comparisons give us some confidence that the colour parameter space spanned by the predicted spiral population in GALICS is consistent with observations for a wide range of redshifts.

3.1 The luminosity function of spiral progenitors

We begin by studying the luminosity function (LF) of spiral progenitors. We are interested in studying how the luminosities of spiral progenitors compare to the general spiral population and what fraction of spirals, at a given luminosity, are early-type progenitors. In Figure 9 we show the evolution of the B-band LF of spiral progenitors - we also show the spiral progenitors separated by the environment of their present-day early-type remnant. The left hand column illustrates the evolution of the spiral LFs - the yellow curve denotes the LF of the general spiral population and the black curve the LF of all spiral progenitors. The LFs of spiral progenitors whose early-type remnants are, at $z = 0$, in clusters, groups and the field, are shown in red, green and blue respectively. Figures 10 and 11 show the corresponding

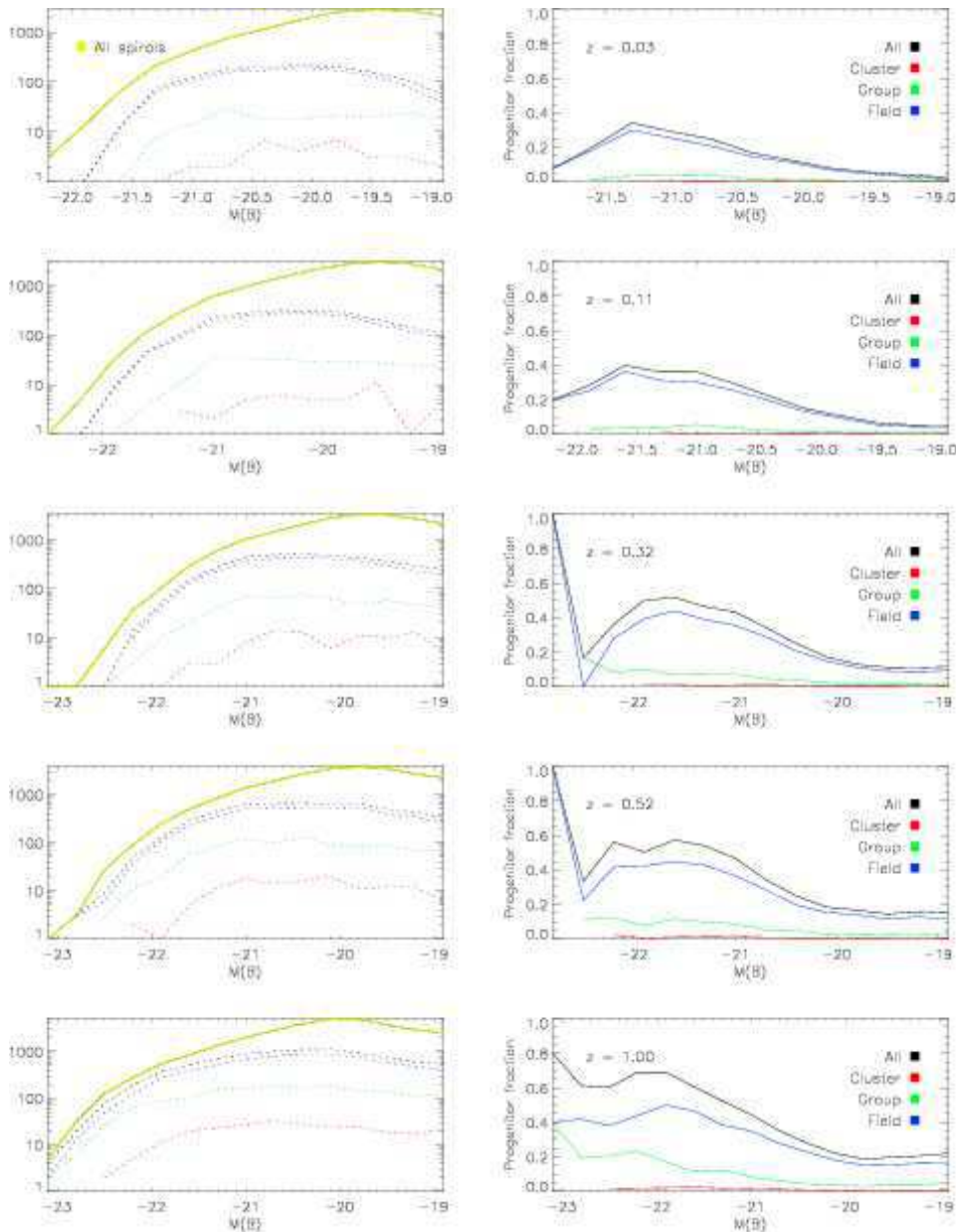


Figure 9. The B-band luminosity function of spiral progenitors.

plots for the predicted V -band and K -band photometry respectively.

It is apparent that there is a greater preponderance of progenitors among larger spirals at all redshifts. For example, at low redshifts ($z < 0.1$), 20 to 40 percent of spirals with $M(B) < -20.5$ are early-type progenitors. At intermediate redshifts ($0.3 < z < 0.52$), these values rise to 30 and 60 percent respectively. At high redshift ($z \sim 1$) spirals with $M(B) < -21.5$ have more than a 60 percent probability of being an early-type progenitor, while spirals with $-20 < M(B) < -21.5$ have between a 30 and 40 percent chance of being early-type progenitors. The falling progenitor fractions towards lower redshift are partly due to the changing morphological mix of the Universe.

3.2 The colour magnitude space of spiral progenitors

While investigating the LFs of spiral progenitors is useful in indicating the *probability* that a spiral of a given luminosity has of being a progenitor, it is also desirable to explore the colour-magnitude (CM) space of the spiral population, so that we can separate progenitor spirals better from the general population at a given luminosity.

In Figure 12 we compare the $(B - V)$ colours of the general spiral population to the $(B - V)$ colours of spiral progenitors. The left-hand column shows the spiral $(B - V)$ CMR from $z = 0$ to $z = 1$. Black dots represent the spiral galaxies and red dots represent spiral progenitors. In the right hand column we show the fraction of spiral progenitors across the $(B - V)$ CMR. The fractions are indicated

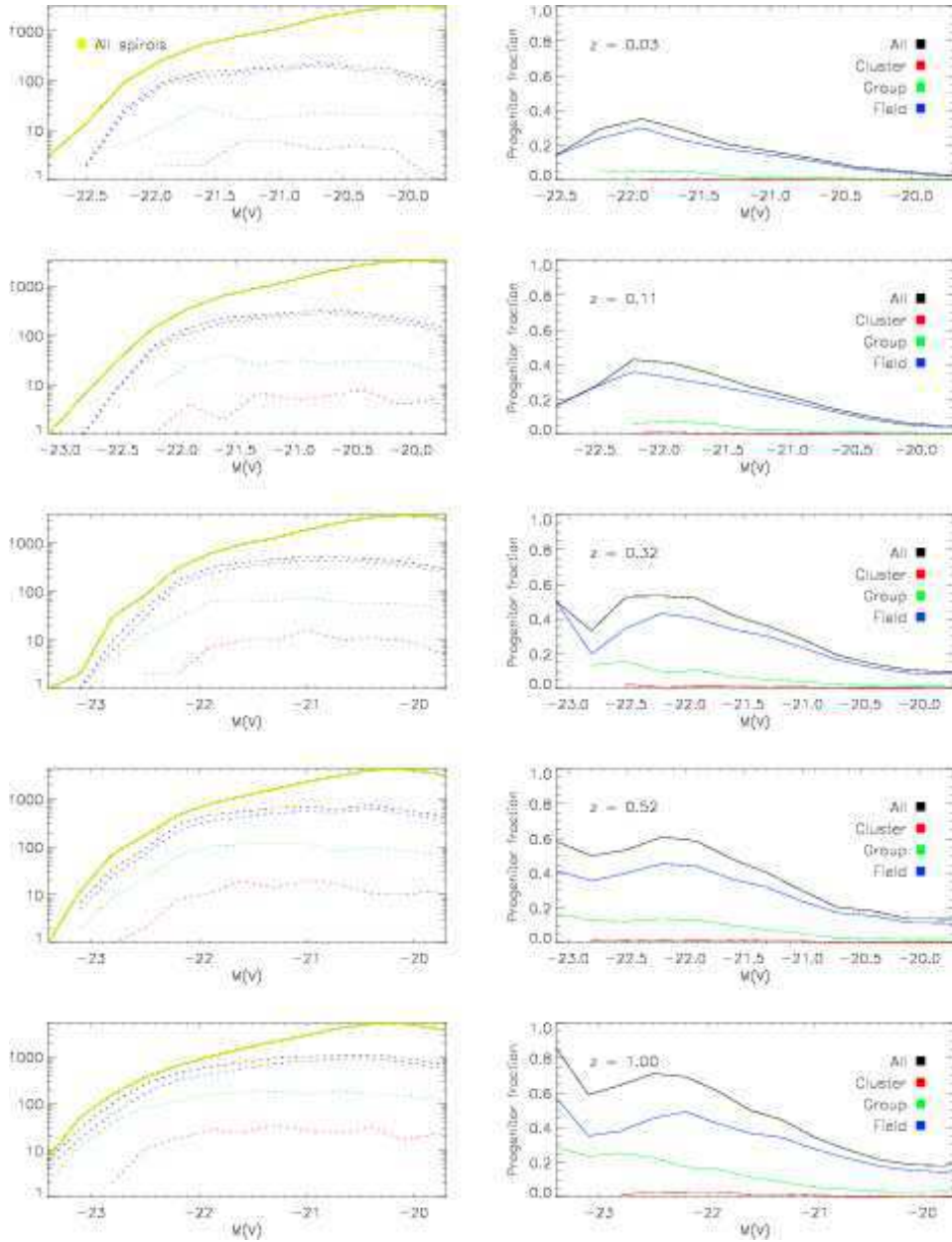


Figure 10. Same as Figure 10 but for the V-band.

using the colour coding shown in the legend. Warmer colours indicate a higher progenitor fraction (red implies a progenitor fraction of 1, black represents a progenitor fraction of 0 and parts of the CM space without any galaxies are not colour-coded).

At local redshifts ($z \sim 0.03$), spirals brighter than $M(B) \sim -21$ have ~ 30 percent chance of being an early-type progenitor, irrespective of their $(B - V)$ colour. At $z \sim 0.1$, spirals with $-21.5 < M(B) < -20.5$ have ~ 30 percent chance of being a progenitor. For larger spirals, those with red $(B - V)$ colours, i.e. $(B - V) > 0.8$, have ~ 60 percent chance of being a progenitor, while the corresponding probability for bluer spirals is 30 to 50 percent.

At intermediate redshift ($z \sim 0.5$), red spirals, with $-21.5 < M(B) < -20.5$ and $(B - V) > 0.6$, have ~ 30

percent probability of being an early-type progenitor, while blue spirals in the same luminosity range have a low progenitor probability. For larger spirals at these redshifts, the probabilities are appreciably higher - red spirals with $(B - V) > 0.7$ have between a 75 and 95 percent chance of being progenitors, while 50 to 75 percent of blue spirals in this luminosity range are progenitors. The situation at high redshift $z \sim 1$ is similar to that at intermediate redshift. For completeness we also show, in Figure 13, the corresponding plot for the $(V - K)$ colours for the spiral population - the trends are similar to those we have just described in $(B - V)$.

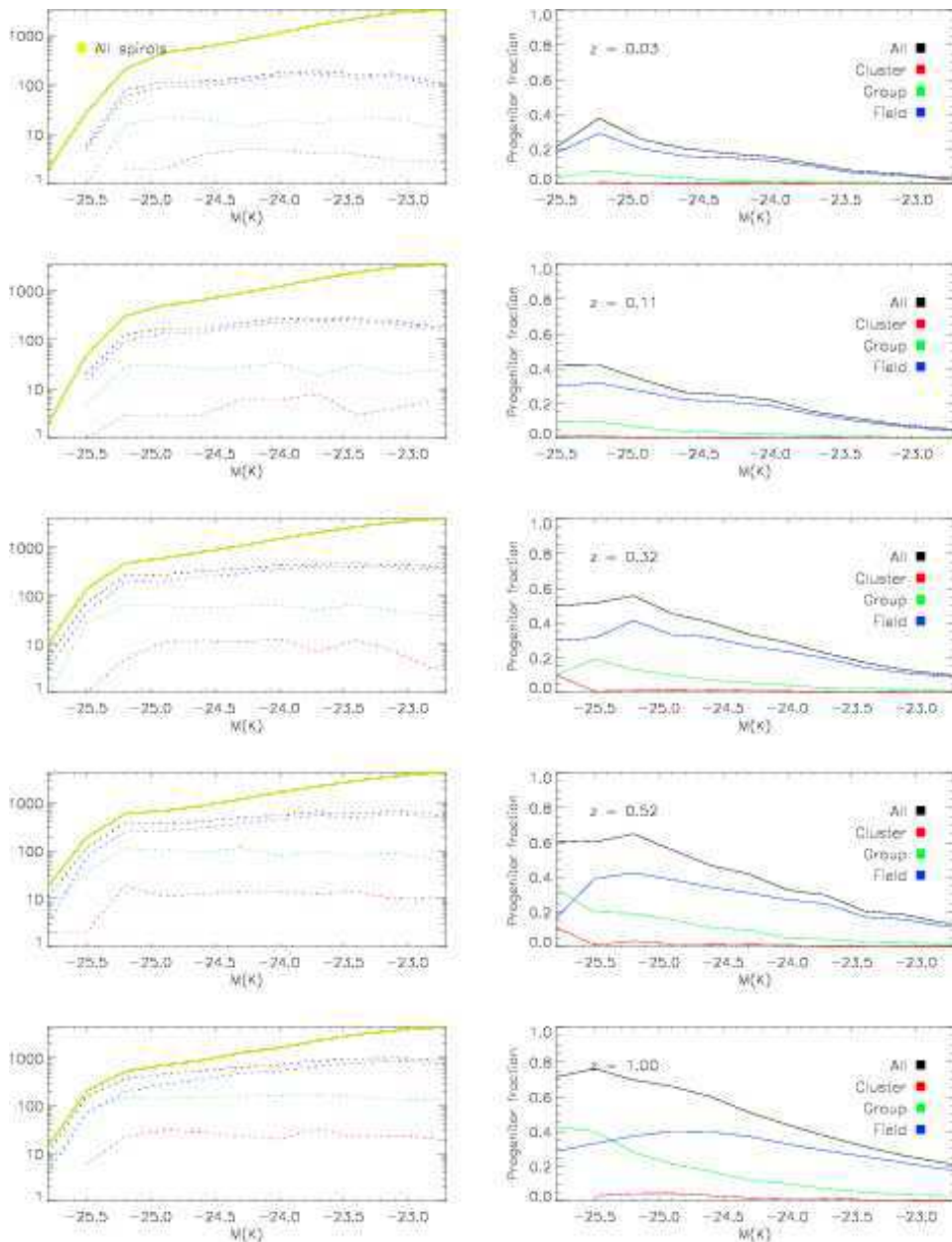


Figure 11. Same as Figure 11 but for the K -band.

4 PROGENITOR EVOLUTION IN CLUSTERS

Before the advent of large scale surveys, dense regions of the Universe were often targetted for early-type galaxy studies, both at low and high redshift (e.g. Bower et al. 1992; Stanford et al. 1998; van Dokkum et al. 1998, 1999, 2000, 2001; Blakeslee et al. 2003). While studies of dense regions are attractive for a variety of reasons (e.g. Ellis 2002; van Dokkum 2004), a key benefit is observational (statistical) convenience - clusters provide access to large homogeneous samples of luminous objects at all redshifts. It has been usual to ‘connect’ results from cluster studies over large redshift ranges to determine (at least qualitatively) the chronology of galaxy evolution.

In this section we investigate progenitors of present-day

cluster early-types, which are themselves in *dense* regions at $z > 0$. The motivation for this investigation is two fold. Firstly (and most importantly), it provides a comparison to the vast literature of ‘cluster’ early-type studies. Secondly, this version of the GALICS model has been accurately calibrated to match the optical CMRs of early-types in *dense* regions from low to high redshift (Kaviraj et al. 2005), which implies that the colours of early-type *progenitors* are also reasonably well constrained. In short, the GALICS model reproduces the optical colours of cluster early-types at $z = 0$ and the colours of all progenitors (regardless of morphology) *in dense regions* at high redshift. Hence, our analysis of the evolution of the *complete* progenitor set (i.e. not just spirals as was studied in the previous section), restricted to dense regions, is likely to be robust.

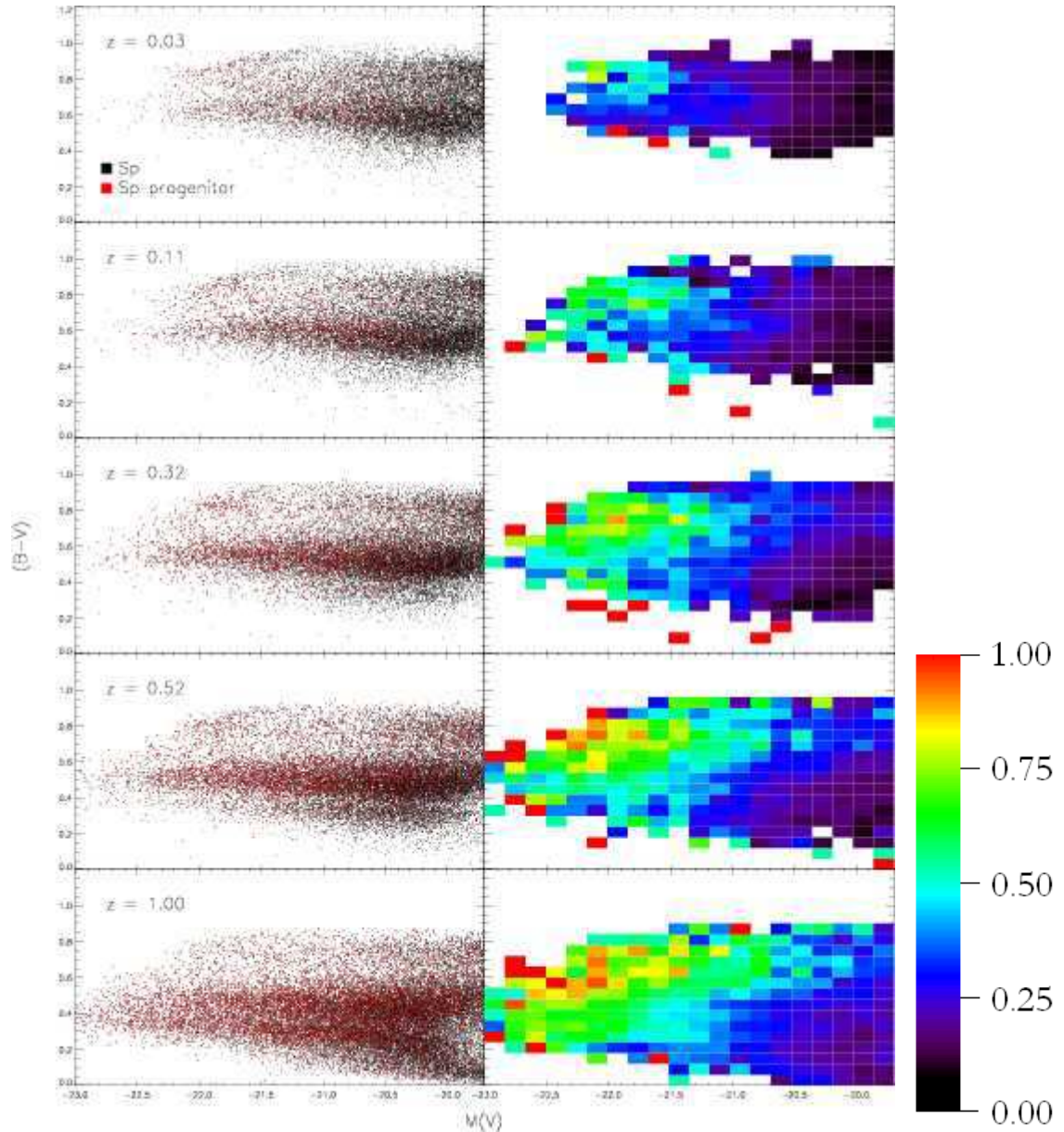


Figure 12. $(B - V)$ colours of the general population compared to the $(B - V)$ colours of those spirals which are progenitors of present-day early-type galaxies. Black dots represent spiral galaxies and red dots represent spiral progenitors. The left-hand column shows the spiral $(B - V)$ CMR from $z = 0$ to $z = 1$. In the right hand column we show the fraction of spirals in parts of the $(B - V)$ CMR space which are progenitors of early-type galaxies. The fractions are indicated using the colour coding shown in the legend. Warmer colours indicate a higher progenitor fraction (red implies a progenitor fraction of 1, black represents a progenitor fraction of 0 and parts of the CM space without any galaxies are not colour-coded).

It is important here to clarify the definitions of ‘density’ that we use to define both ‘clusters’ at present-day, and ‘dense’ regions at high redshift. As mentioned before, model ‘density’ is assumed to be a direct function of the mass of the DM halo in which galaxies are embedded. At $z = 0$, a DM halo mass of $10^{14} M_{\odot}$ represents the lower limit for a cluster-hosting halo. Observational studies of dense regions at high redshift are likely to contain an assortment of cluster-type haloes of varying occupancies. Furthermore, DM haloes themselves are evolving - on average, the largest

haloes at $z = 1$ are likely to be roughly half their size at present day (e.g van den Bosch 2002). To take these two points into account, we use a *variable* lower mass limit for ‘cluster-hosting’ haloes at $z > 0$. At a given redshift this lower limit is calculated from the average mass accretion history (van den Bosch 2002, see their Figure5) applied to a $10^{14} M_{\odot}$ halo.

Figure 14 shows the $(B - V)$ CMR in clusters in the redshift range $0 < z < 1$. Large diamonds indicate progenitor galaxies - black indicates ellipticals, green corresponds

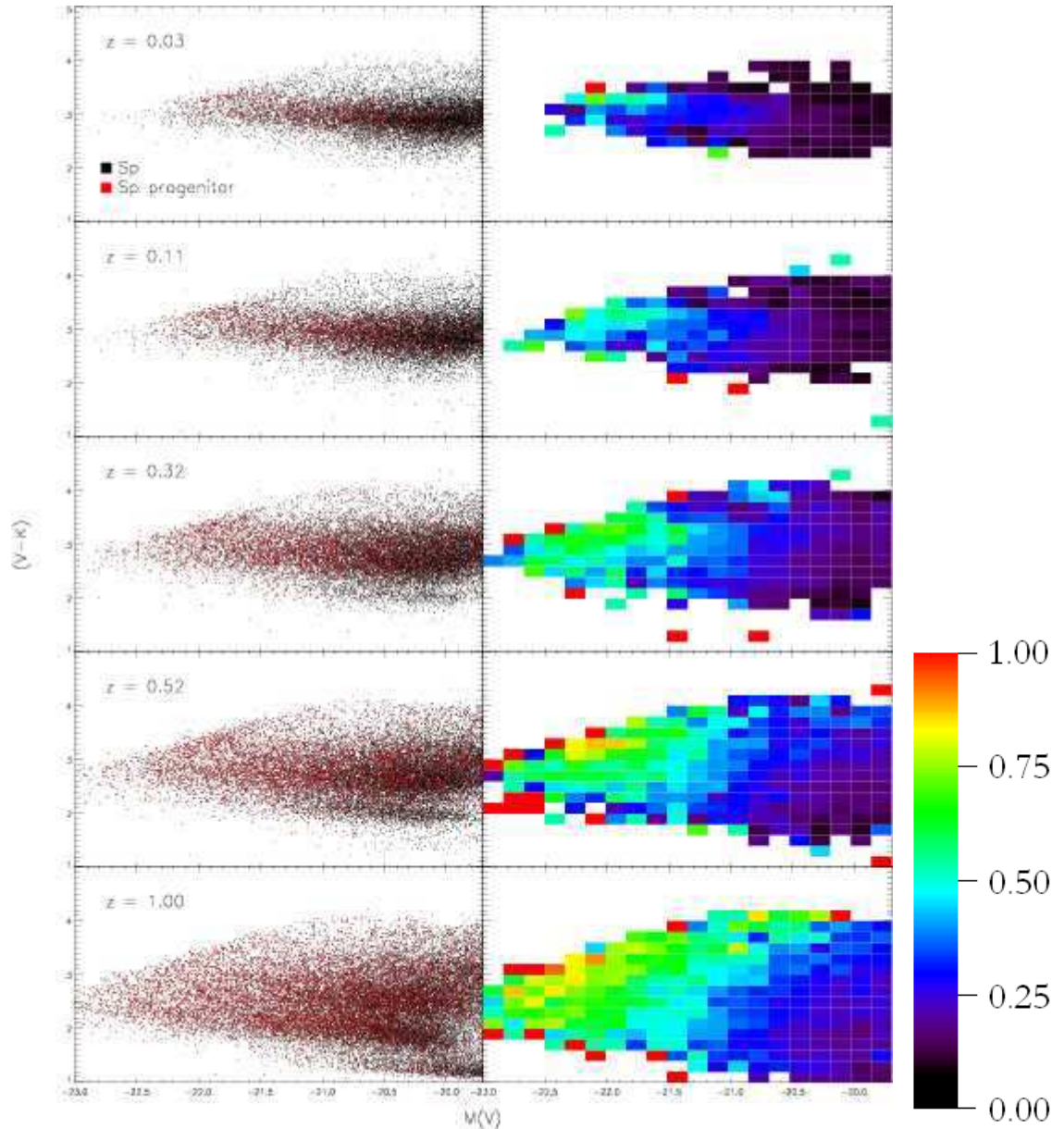


Figure 13. $(V - K)$ colours of the general population compared to the $(V - K)$ colours of those spirals which are progenitors of present-day early-type galaxies. Black dots represent spiral galaxies and red dots represent spiral progenitors. The left-hand column shows the spiral $(V - K)$ CMR from $z = 0$ to $z = 1$. In the right hand column we show the fraction of spirals in parts of the $(V - K)$ CMR space which are progenitors of early-type galaxies. The fractions are indicated using the colour coding shown in the legend. Warmer colours indicate a higher progenitor fraction (red implies a progenitor fraction of 1, black represents a progenitor fraction of 0 and parts of the CM space without any galaxies are not colour-coded).

to S0s and blue indicates spiral galaxies. Small dots indicate galaxies which do not contribute to the mass in present-day cluster early-types. All early-type galaxies in dense regions are, not unexpectedly, progenitors of cluster early-types at present day. The top panel in Figure 15 shows the fraction of spiral galaxies in dense regions at high redshift (split by luminosity) which are progenitors of early-types at $z = 0$. The bottom panel shows the offset in $(B - V)$, with respect to elliptical progenitors, of the S0 and spiral progenitor galaxies. The offsets are shown split by luminosity.

We find that at high redshift ($z \sim 1$) up to 40 percent of large spirals ($-23 < M(V) < -21$) are progenitors, whereas only ~ 10 percent of small spirals ($M(V) > -21$) are members of the progenitor set. Large spirals are four times more likely to be progenitors than small spirals, regardless of redshift, in the redshift range $0 < z < 1$. Elliptical galaxies form the reddest locus in $(B - V)$. S0 galaxies show an average offset of -0.04 compared to the elliptical population, regardless of luminosity. Large spiral progenitors show an average $(B - V)$ offset of -0.05 compared to the elliptical

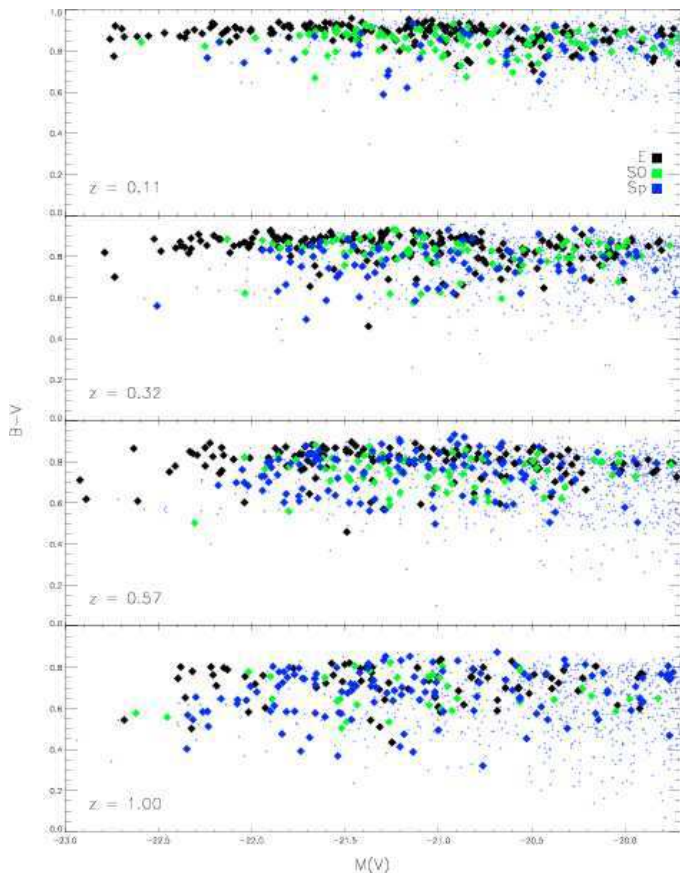


Figure 14. The $(B - V)$ CMR in clusters in the redshift range $0 < z < 1$. Large diamonds indicate the progenitors of present-day cluster early-type galaxies. Small dots indicate galaxies which do not contribute to the mass in present-day cluster early-types. Note that all elliptical and S0 galaxies in dense regions are, not unexpectedly, progenitors of present-day cluster early-types.

population at high redshift, mainly because the scatter in the elliptical colours also tends to be large at high redshift. At low redshift the offset is more pronounced - large spiral progenitors are upto 0.1 mags bluer in $(B - V)$ than the elliptical population.

5 THE ‘RED SEQUENCE’ AS A PROXY FOR THE PROGENITOR SET

Early-type galaxies in clusters tend to preferentially populate the reddest parts of the CM space. In this section we investigate whether the sample of galaxies (without reference to morphology), within the ‘red sequence’ defined by the early-type population, can be used as a proxy for the progenitor set. We define the red sequence as the galaxy population which occupies the part of the CM space ‘dominated’ by early-type galaxies. In Figures 16 and 17 the CM space dominated by early-type galaxies is shown in grey - this region is determined by a progressive one-sigma fit to the colours of the early-type population. It therefore contains, on average, 68 percent of the early-type population within it. Large diamonds indicate galaxies which are part of the progenitor set. Galaxies which are not part of the

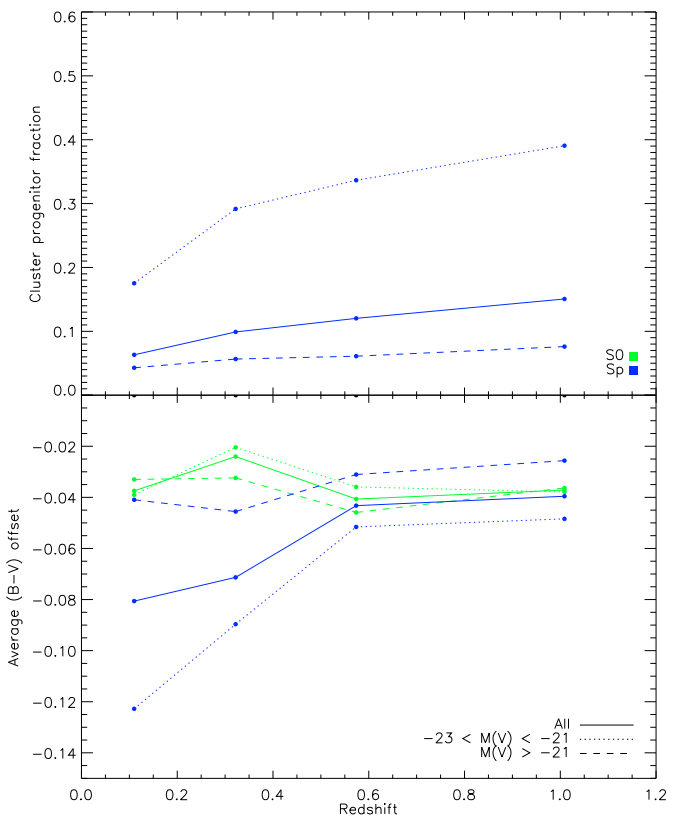


Figure 15. TOP PANEL: The fraction of spiral galaxies in dense regions at high redshift (split by luminosity) which are progenitors of cluster early-types at $z = 0$. BOTTOM PANEL: The offset in the $(B - V)$, with respect to elliptical progenitors, of S0 and spiral progenitors in clusters. The offsets are shown split by luminosity.

progenitor set are shown using small crosses. Galaxies in the red sequence are circled. It is apparent that the red sequence misses blue progenitor galaxies, both early-type and late-type. Figure 16 shows the evolution of the ‘red sequence’ from low to intermediate redshift and Figure 17 the evolution from intermediate to high redshift.

In Figure 18 we compare galaxies in the actual progenitor set to those in the red sequence. The top panel shows the number ratio between the progenitor set population and the red sequence population, split by redshift and luminosity, while the bottom panel shows the mass ratio between the progenitor set population and the red sequence population split by redshift and luminosity. It is apparent that large galaxies ($-23 < M(V) < -21$) in the red sequence trace the progenitor set well in terms of number and mass but that the relationship breaks down as we go towards the lower end of the luminosity function ($M(V) > -21$). The number and mass fractions remain stable, as a function of the luminosity slices shown in Figure 18, within the redshift range explored in this study ($0 < z < 1$).

Luminosity evolution studies which use the red sequence as a proxy for the early-type population (e.g. Bell et al. 2004) can therefore achieve accurate results *only* for the upper end of the luminosity function. However, the red sequence should not be used as a proxy for the progenitor set further down

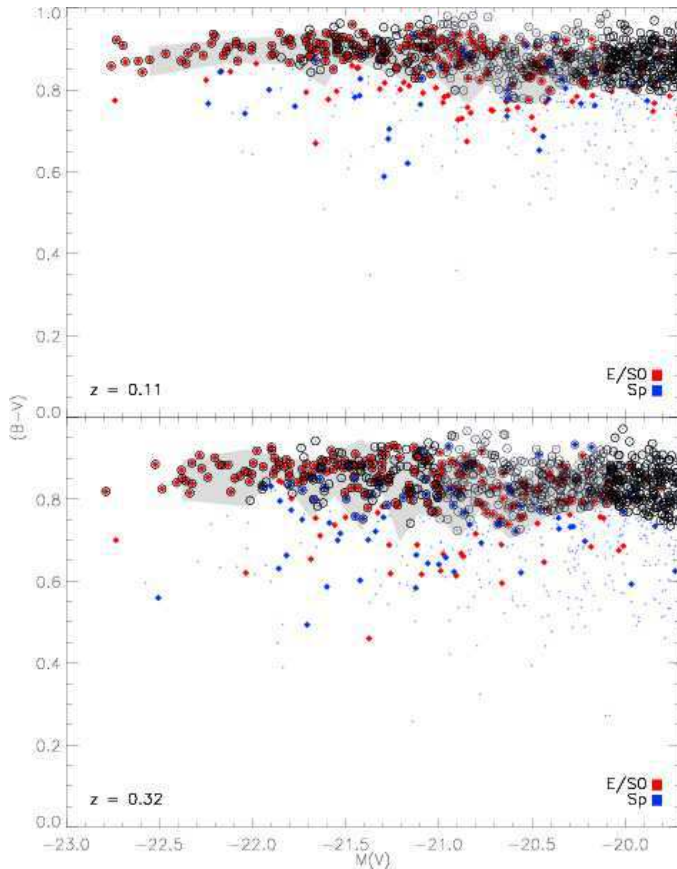


Figure 16. The composition of the ‘red sequence’, defined as the galaxy population which occupies the part of the CM space dominated by early-type galaxies (shown in grey), compared with the progenitor set in cluster populations. The diamonds indicate galaxies which are part of the progenitor set. Galaxies which are not part of the progenitor set are shown using small crosses. Galaxies in the red sequence are circled. The ‘red sequence’ misses blue galaxies, both early-type and late-type. This plot shows the evolution of the ‘red sequence’ from low to intermediate redshift.

the luminosity function, since a larger fraction of the (spiral) red sequence does not contribute to the progenitor set. In addition, the red sequence, almost by definition, misses contributions due to early-types which lie blueward of it. This is increasingly true at higher redshift - hence conclusions based on the colours of the red sequence should *not* generally be applied to early-type evolution.

6 CONCLUSIONS

We have comprehensively explored the extent of progenitor bias as a function of the luminosity and environment of the early-type remnant at $z = 0$. Our study, using the GALICS semi-analytical model, is the first of its kind which uses a fully realistic semi-analytical framework, in which mass assembly and morphological transformation can be followed accurately in the context of the currently popular hierarchical merger paradigm. Against the backdrop of the impending or recent release of data from large-scale surveys *at high redshift*, the results of this study are timely, providing a pic-

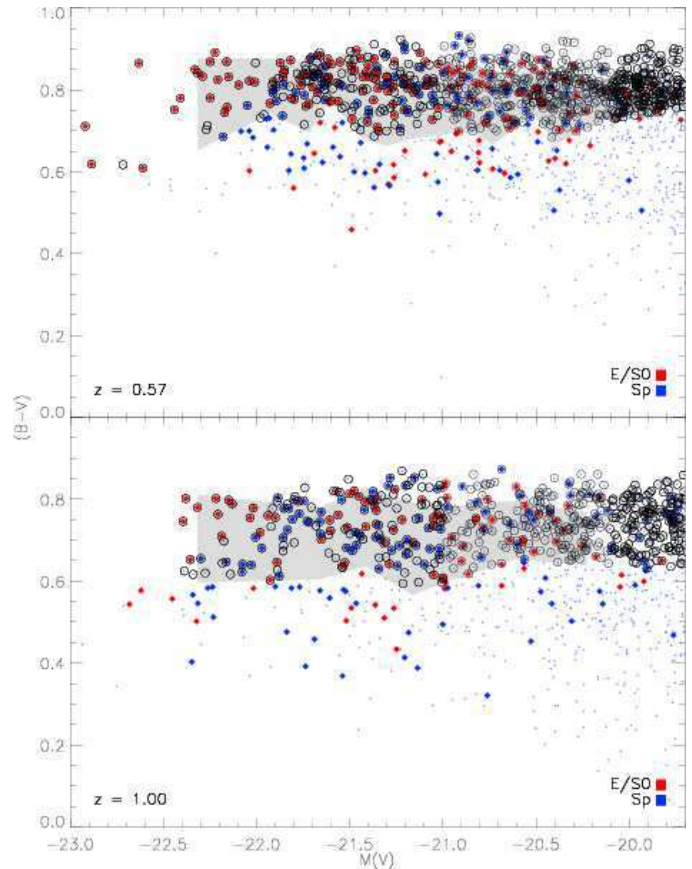


Figure 17. The composition of the ‘red sequence’, defined as the galaxy population which occupies the part of the CM space dominated by early-type galaxies (shown in grey), compared with the progenitor set in cluster populations. The diamonds indicate galaxies which are part of the progenitor set. Galaxies which are not part of the progenitor set are shown using small crosses. Galaxies in the red sequence are circled. The ‘red sequence’ misses blue galaxies, both early-type and late-type. This plot shows the evolution of the ‘red sequence’ from intermediate to high redshift.

ture of the mass assembly in present-day early-types and gauging the extent by which progenitor bias may affect the conclusions from ‘early-type only’ studies at high redshift.

The main conclusions from our study can be summarised as follows:

- Larger early-types in all environments are *assembled later* than their less massive counterparts. However, their stellar populations are generally older (Kaviraj et al. 2005).
- On average, without reference to environment, only 35 percent of early-type galaxies are in place by $z = 1$. Morphological transformations are significantly faster in cluster environments (where the vast majority of early-type studies have been based before the advent of large-scale surveys). In clusters almost 70 percent of early-types are in place by $z = 1$. In other words, the probability of a ‘major merger’, which creates an early-type remnant is low after $z = 1$ in cluster type environments.
- Averaging across all environments, at $z \sim 1$, less than 50 percent of the stellar mass which ends up in early-types today is actually in early-type progenitors at this redshift. This value is around 65 percent in clusters owing to faster

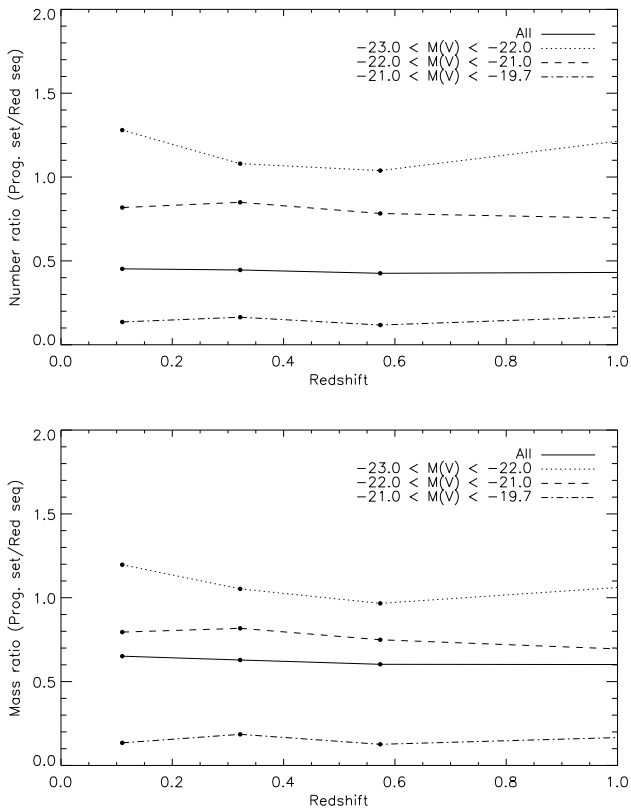


Figure 18. Comparison between galaxies in the actual progenitor set to those in the red sequence. TOP: Number ratio between the progenitor set population and the red sequence population split by redshift and luminosity. BOTTOM: Mass ratio between the progenitor set population and the red sequence population split by redshift and luminosity. It is apparent that large galaxies in the red sequence trace the progenitor set well in terms of number and mass but that the relationship breaks down rather rapidly as we go towards the lower end of the luminosity function.

morphological transformation in this environment. In other words, looking *only* at early-type progenitors does not take into account almost half the mass in the progenitor set - the progenitor set doubles in mass in the redshift range $0 < z < 1$.

- Progenitor bias does not arise simply because (late-type) progenitor mass is missed, but also because the age profile of mass in progenitors of different morphological types tend to vary. Spiral progenitors are typically ‘bluer’ because they host more recently formed stars than early-type progenitors. Hence, age-dating the progenitor set using an ‘early-type only’ CMR after excluding the spiral progenitors biases the CMR towards redder colours and *overestimates* the average of the population.

- One of the principal aims of this study is to provide a means of *including* spiral progenitors which might be early-type progenitors, and thus correct, at least partially, for progenitor bias. We have therefore focussed on spiral progenitors in the model and compared their properties, in detail, to the general spiral population.

- There is a greater preponderance of progenitors among larger spirals at all redshifts. At low redshifts ($z < 0.1$),

20 to 40 percent of spirals with $M(B) < -20.5$ are early-type progenitors. At intermediate redshifts $0.3 < z < 0.5$, these values rise to 30 and 60 percent respectively. At high redshift ($z \sim 1$) spirals with $M(B) < -21.5$ have more than a 60 percent probability of being an early-type progenitor while spirals with $-20 < M(B) < -21.5$ have between a 30 and 40 percent chance of being early-type progenitors. The falling progenitor fractions towards lower redshift are partly due to the changing morphological mix of the Universe.

- The colour-magnitude space of the spiral population provides a better route to identifying spiral progenitors using both the luminosity and the optical colour. At $z \sim 0.1$, spirals with $-21.5 < M(B) < -20.5$ have ~ 30 percent chance of being a progenitor. For larger spirals, those with red ($B - V$) colours, i.e. $(B - V) > 0.8$, have ~ 60 percent chance of being a progenitor, while the corresponding probability for bluer spirals is 30 to 50 percent.

At intermediate redshift ($z \sim 0.5$), *red* spirals, with $-21.5 < M(B) < -20.5$ and $(B - V) > 0.6$, have ~ 30 percent probability of being an early-type progenitor, while blue spirals in the same luminosity range have a low progenitor probability. For larger spirals at these redshifts, the probabilities are appreciably higher - red spirals with $(B - V) > 0.7$ have between a 75 and 95 percent chance of being progenitors, while 50 to 75 percent of blue spirals in this luminosity range are progenitors. The situation at high redshift $z \sim 1$ is similar to that at intermediate redshift. The trends in the $(V - K)$ colour are similar to those in $(B - V)$.

- Finally we have explored the correspondence between the progenitor set and the ‘red sequence’, defined as the part of the CM parameter space which is dominated by early-type galaxies. We find that galaxies, both late and early-type, that fall in this parameter space do not necessarily trace the progenitor set well. Large galaxies ($-23 < M(V) < -21$) in the red sequence correspond to the progenitor set reasonably well in terms of number and mass but the relationship breaks down as we go towards the lower end of the luminosity function ($M(V) > -21$). Hence, luminosity evolution studies which use the red sequence as a proxy for the early-type population, therefore achieve accurate results only for the upper end of the luminosity function. In addition, the red sequence, almost by definition, misses contributions due to early-types which lie blueward of it - hence conclusions based on the colours of the red sequence should not generally be applied to early-type evolution, *especially at high redshift*.

REFERENCES

- Baugh, C. M., S. Cole, and C. S. Frenk (1996). *MNRAS* 283, 1361–1378.
- Bell, E. F. and GEMS collaboration (2004). *ApJ* 608, 752–767.
- Blakeslee, J. P., M. Franx, M. Postman, P. Rosati, B. P. Holden, G. D. Illingworth, H. C. Ford, N. J. G. Cross, C. Gronwall, N. Benítez, R. J. Bouwens, T. J. Broadhurst, M. Clampin, R. Demarco, D. A. Golimowski, G. F. Hartig, L. Infante, A. R. Martel, G. K. Miley, F. Menanteau, G. R. Meurer, M. Sirianni, and R. L. White (2003). *ApJ* 596, L143–L146.

- Bower, R. G., J. R. Lucey, and R. Ellis (1992). *MNRAS* 254, 589.
- Buta, R., S. Mitra, G. de Vaucouleurs, and H. G. Corwin (1994). *AJ* 107, 118–134.
- Cross, N., S. P. Driver, W. Couch, C. M. Baugh, J. Bland-Hawthorn, T. Bridges, R. Cannon, S. Cole, M. Colless, C. Collins, G. Dalton, K. Deeley, R. De Propris, G. Efstathiou, R. S. Ellis, C. S. Frenk, K. Glazebrook, C. Jackson, O. Lahav, I. Lewis, S. Lumsden, S. Maddox, D. Madgwick, S. Moody, P. Norberg, J. A. Peacock, B. A. Peterson, I. Price, M. Seaborne, W. Sutherland, H. Tadros, and K. Taylor (2001). *MNRAS* 324, 825–841.
- Ellis, R. S. (2002). In *ASP Conf. Ser. 268: Tracing Cosmic Evolution with Galaxy Clusters*, pp. 311–+.
- Hatton, S., J. E. G. Devriendt, S. Ninin, F. R. Bouchet, B. Guiderdoni, and D. Vibert (2003). *MNRAS* 343, 75–106.
- Kaviraj, S., J. E. G. Devriendt, I. Ferreras, and S. K. Yi (2005). *MNRAS* 360, 60–68.
- Martin, D. C. and GALEX Team (2005). *ApJ* 619, L1–L6.
- Simien, F. and G. de Vaucouleurs (1986). *ApJ* 302, 564–578.
- Stanford, S. A., P. R. Eisenhardt, and M. Dickinson (1998). *ApJ* 492, 461–+.
- van den Bosch, F. C. (2002). *MNRAS* 331, 98–110.
- van Dokkum, P. (2004). In *Wide-Field Imaging From Space*.
- van Dokkum, P. G. and M. Franx (1996). *MNRAS* 281, 985–1000.
- van Dokkum, P. G. and M. Franx (2001). *ApJ* 553, 90–102.
- van Dokkum, P. G., M. Franx, D. Fabricant, G. D. Illingworth, and D. D. Kelson (2000). *ApJ* 541, 95–111.
- van Dokkum, P. G., M. Franx, D. Fabricant, D. D. Kelson, and G. D. Illingworth (1999). *ApJ* 520, L95–L98.
- van Dokkum, P. G., M. Franx, D. D. Kelson, and G. D. Illingworth (1998). *ApJ* 504, L17+.
- van Dokkum, P. G., S. A. Stanford, B. P. Holden, P. R. Eisenhardt, M. Dickinson, and R. Elston (2001). *ApJ* 552, L101–L104.
- Wolf, C., K. Meisenheimer, M. Kleinheinrich, A. Borch, S. Dye, M. Gray, L. Wisotzki, E. F. Bell, H.-W. Rix, A. Cimatti, G. Hasinger, and G. Szokoly (2004). *A&A* 421, 913–936.